Original Article

Neurogenic marker expression in differentiating human adipose derived adult mesenchymal stem cells

Neus Gomila Pelegri[1,2], Bruce K. Milthorpe[1], Catherine A. Gorrie[2], Jerran Santos[1]

[1]Advanced Tissue Engineering and Stem Cell Biology Group, School of Life Sciences, University of Technology Sydney, Sydney, NSW, Australia; [2]Neural Injury Research Unit, School of Life Sciences, University of Technology Sydney, Sydney, NSW, Australia

Contributions: (I) Conception and design: J Santos, BK Milthorpe, NG Pelegri; (II) Administrative support: CA Gorrie; (III) Provision of study materials: J Santos; (IV) Collection and assembly of data: NG Pelegri; (V) Data analysis and interpretation: NG Pelegri; (VI) Manuscript writing: All authors; (VII) Final approval of manuscript: All authors.

Correspondence to: Jerran Santos, PhD. Advanced Tissue Engineering and Stem Cell Biology Group, School of Life Sciences, University of Technology Sydney, Sydney, NSW, Australia. Email: Jerran.Santos@uts.edu.au.

Background: Adipose-derived stem cells (ADSCs) are increasingly utilised in the field of neural regeneration due to their high accessibility and capacity for differentiation into neural like cells. Culturing ADSCs in the presence of various growth factors, small molecules and combinations thereof have shown promise in this regard; however, these protocols are generally complex, time-consuming and costly. The need for commercially available and chemically defined growth media/supplements is required to facilitate further developments in this area.

Methods: In this study, we have examined the neural differentiation and proliferation potential of the commercially available supplements B27, CultureOne (C1) and N2 on human ADSCs (hADSCs). Through a combination of immunocytochemistry, cytokine analysis, and CNPase enzymatic assays, we provide novel insight into the neural differentiation effects of B27, C1 and N2 on hADSCs.

Results: The study found that C1 and N2 supplements initiated neural differentiation of the cells, with C1 pushing differentiation towards an oligodendrocytic lineage and N2 initiating neuronal differentiation. This suggests that C1 and N2 supplements can be used to drive neural differentiation in hADSCs. However, B27 did not show significant differentiation in the time frame in which the experiments took place and therefore is unsuitable for this purpose.

Conclusions: These findings highlight the utility of commercially available supplements in the neural differentiation of ADSCs and may assist in establishing simpler, more affordable differentiation protocols.

Keywords: CNPase; neurogenesis; oligodendrocytes; neurons; adipose-derived stem cells (ADSCs)

Received: 21 June 2022; Accepted: 16 February 2023; Published online: 23 March 2023.

doi: 10.21037/sci-2022-015

View this article at: https://dx.doi.org/10.21037/sci-2022-015

Introduction

Adipose-derived stem cells (ADSCs), a mesenchymal stem cell (MSC) type, are of particular interest given that they are multipotent *in vitro* and are easily obtained via subcutaneous adipose tissue liposuction. This is a less invasive procedure compared to other common stem cell collection methods like bone marrow aspirates but still yields high cell numbers (1-6). ADSCs have the potential to differentiate into adipogenic, chondrogenic, osteogenic, myogenic, and neurogenic like cell lineages (7-10), making them suitable for many applications. Additionally, ADSCs have also been found to express b-III tubulin and NeuN in their undifferentiated state, two well-known markers of neuronal differentiation, hinting at their potential to become neural-like cells (11).

The differentiation of ADSCs into neural-like cells challenges the dogma that adult stem cells are multipotent and are restricted to differentiating into cell types derived

from the same embryonic germ layer; ADSCs are derived from the mesoderm while neural cells are derived from the ectoderm (12,13). Stem cell phenotypic signatures can be mapped out through several analytical techniques. These result in the identification of molecular and cellular markers, including surface makers, secreted proteins, and cytokines. These types of analyses highlight aspects of the cells' differentiation potential, while others suggest functions of specific molecules during the various differentiation states. To date, several different growth factors and chemicals have been explored to induce neural differentiation in ADSCs; rodent ADSCs have been successfully differentiated into neural stem cells (NSCs) and dopaminergic neurons following a two-step protocol of overnight pre-induction with basic fibroblast growth factor (bFGF), butylated hydroxyanisole (BHA), and B27 supplement followed by a 14-day treatment with sonic hedgehog (SHH), fibroblast growth factor 8 (FGF8) and B27 supplement over 14 days (14).

Human ADSCs (hADSCs) have been successfully differentiated towards neuronal lineages and into neurospheres by using a mixture of B27 supplement, bFGF and human epidermal growth factor (hEGF) for a week and then further differentiated into neuron-like cells by following treatment with a mixture of by L-glutamine, non-essential amino acids, N2 supplement and B27 supplement for another week (15). hADSCs have also been differentiated into dopamine-secreting cells using a growth factor cocktail composed of SHH, bFGF, FGF8, and brain derived neurotrophic factor (BDNF) in low-serum conditions (16) and in B27 supplemented serum-free conditions (17). Neural differentiation in hADSCs has also been induced with valproic acid (18) and isobutylmethyl xanthine (IBMX) (19). MSCs have also shown to differentiate towards neural stem cells (NSCs) and neurons and increase the secretion of BDNF and nerve growth factor (NGF) when co-cultured with NSCs (20). Additionally, ADSC transplants with or without prior differentiation have been reported to be beneficial in animal models of neuronal disorders such as Parkinson's disease, (21) peripheral nerve injury (22), epilepsy (23) and stroke (24), indicating their neuroregenerative potential.

A great variety of growth factors and chemicals are being studied alone or in combination as potential protocols for hADSCs differentiation into neural-like cells. Here, we will explore three readily available media supplements in isolation to distinguish the effects of the supplements on the hADSC differentiation process. In this current study, the potential of B27, CultureOne (C1) and N2 will be examined for neural differentiation of hADSCs *in vitro* using microscopic analysis to track morphological changes and cell numbers, immunocytochemistry to detect changes in neural marker expression and Bioplex analysis to investigate the changes in cytokine and chemokine secretion levels by the cells. Cytokines and chemokines investigation provides valuable insight into the secreted cytokines and their role in activating differentiation pathways in cells (25). As per the manufacturer's descriptions, these are commercially available neural differentiation and proliferation supplements and have been used for maintenance, maturation, proliferation and differentiation of neuronal stem cells (26,27).

Methods

Cell culture

Maintenance

hADSCs from a single donor were isolated and expanded as previously described (28) with approval from the UTS Human Research Ethics Committee (Ethics No. 2013000437). The study was conducted in accordance with the Declaration of Helsinki (as revised in 2013). Written informed consent was acquired for donor lipoaspirate release for research purposes only. After isolation, hADSCs were maintained in control media [Dulbecco's Modified Eagle medium (DMEM)/F12 + Glutamax media] (Gibco, Life Technologies, Carlsbad, CA, USA) with 10% heat inactivated foetal bovine serum (FBS, Gibco, Life Technologies, Carlsbad, CA, USA) and 1% Antibiotics/Antimycotics (ABAM, Gibco, Life Technologies, Carlsbad, CA, USA) and incubated at 37 ℃ at 5% CO_2. hADSCs were passaged five to seven times post isolation by stripping cells with TrypLE Express (12604 Gibco, Life Technologies, Roskilde, Denmark) before being cryostored by storing the cells in 90% FBS/10% DMSO v/v at –80 ℃.

Differentiation

Cells were revived from cryostorage under sterile conditions at passage 7 into control media DMEM/F12 + Glutamax media with 10% FBS and incubated at 37 ℃ with 5% CO_2. Cells were expanded until passage 9, and when they reached 80% confluency, they were seeded into either 6 well plates at 40,000 cells/mL or 24-well plates at 20,000 cells/mL for molecular or imaging analysis, respectively. Once cells reached 95%±2% confluence, treatment commenced. There were 3 biological replicates.

hADSCs were treated under sterile conditions at all

Table 1 Treatment groups

Treatment	Cell type	Base media	Supplement
B27	hADSC	Neurobasal media	B27 supplement (50×) #17504-001 (Gibco, Life Technologies)
N2	hADSC	Neurobasal media	N2 supplement (100×) #17502-048 (Gibco, Life Technologies)
CultureOne	hADSC	Neurobasal media	CultureOne (C1) supplement (100×) #A33202-01 (Gibco, Life Technologies)
DMEM (undifferentiated control)	hADSC	DMEM/F12 + Glutamax—control media	10% FBS (Gibco, Life Technologies)
Staining controls	SHSY-5Y (NBCs) or U87MG (GBCs)	DMEM/F12 + Glutamax—control media	10% FBS (Gibco, Life Technologies)

DMEM, Dulbecco's Modified Eagle medium; hADSC, human adipose-derived stem cell; FBS, foetal bovine serum; NBC, neuroblastoma cell; GBC, glioblastoma cell.

times, and media were changed every 84 hours for 7 days. All cells were treated with either control media DMEM (DMEM/F12 + Glutamax + 10% FBS) (Gibco, Life Technologies, Carlsbad, CA, USA) or with Neurobasal media (Gibco, Life Technologies, Carlsbad, CA, USA) with 1% abam [antibiotic-antimycotic (100×) #15240-062 Invitrogen, CA, USA] and the addition of supplements shown in *Table 1*. The treatments used are commercially available media supplements for the purpose of neuronal cell maintenance, survival and differentiation *in vitro*. During treatment, at every media change, conditioned media were collected for further testing, and phase images at 10x magnification were taken of each treatment condition on the same marked area using the EVOS XL Core microscope (Thermofisher, Massachusetts, USA).

After 7 days of treatment, cells were either fixed for immunocytochemistry with 10% formalin for 30 min at room temperature, or they were harvested using a cell scraper and frozen at –80 ℃ for further testing.

Cytokine analysis

Bioplex

The Bioplex assay is a commercially available immunoassay kit (Bio-plex Pro human cytokine 27-plex, M50-0KCAF0Y BioRad Laboratories, Hercules, CA, USA) for investigating and quantitating cytokine concentration changes relative to the baseline levels of up to 27 cytokines across multiple sample types simultaneously.

During treatment, 500 µL aliquots of conditioned media from each treatment group were collected at time 0 h and after every 84 h and stored at –80 ℃ until the assay was conducted. Concentrations of 27 cytokines consisting of interlukins IL-1b, IL-1ra, IL-2, IL-4, IL-5, IL-6, IL-7, IL-8, IL-9, IL-10, IL-12, IL-13, IL-15, IL-17A, Eotaxin, fibroblast growth factor (FGF) basic, granulocyte colony-stimulating factor (G-CSF), granulocyte-macrophage colony-stimulating factor (GM-CSF), interferon (IFN)-g, interferon gamma induced protein-10 (IP-10), monocyte chemoattractant protein-1 (MCP-1), macrophage inflammatory protein-1a (MIP-1a), platelet derived growth factor-bb (PDGF-bb), macrophage inflammatory protein-1b (MIP-1b), RANTES, tumor necrosis factor (TNF)-α and vascular endothelial growth factor (VEGF)] were simultaneously assessed using the Bioplex kit. Assays were performed according to the manufacturer's instructions.

Protein analysis

Immunocytochemistry

After a primary wash with phosphate-buffered saline (PBS 0.01 M), fixed cells underwent a second wash step for 15 minutes in phosphate buffered saline triton-x (PBST) [0.01 M PBS and 0.1% Triton X-100 (BDH #30632) at pH 7.4]. They were then blocked in 5% normal goat serum (NGS) (Sigma-Aldrich #G9023) in PBST for 30 minutes. Primary antibodies were diluted in PBG [0.1 M PBS, pH 7.4, 0.1% Triton-X, 2% NGS, 1% bovine serum albumin (BSA) (Sigma-Aldrich #A9647)] and were added to the relevant wells and incubated overnight at room temperature with gentle agitation. Primary antibodies were rabbit anti-glial fibrillary acidic protein (GFAP) (1:1,000, Dako, Denmark #Z0334) as an astrocyte marker; rabbit anti-β-III tubulin (1:500, Abcam, Cambridge, UK #ab18207) as an

early neuronal marker; mouse anti-CNPase (1:200 Abcam, #ab6319-100) as an oligodendrocyte marker; rabbit anti-Ki67 (1/50 Abcam, #ab833) as a proliferation marker; and rabbit anti-DoubleCortin (1:1,000 Abcam, #ab18723) as a neuron developing maker. Cells were then washed with three changes of PBST and incubated with goat anti-mouse AF488 (1:200, Invitrogen, #A11001) or goat anti-rabbit AF488 (1:200, Invitrogen, #A11008) secondary antibodies in PBG for two hours at room temperature with gentle agitation. Following an additional wash with PBST, and counterstained with Hoechst (1:5,000 Invitrogen) for 30 minutes to stain the nuclei and finally washed twice with PBST. Plates were imaged using an IN Cell Analyzer 2200 high-content cellular analysis system (GE Healthcare Life Sciences, UK). Positive staining control cells were included in all staining runs. Glioblastoma U87MG cells were used for GFAP, 2',3' cyclic-nucleotide 3' phosphodiesterase (CNPase), and Ki67 positive staining controls. Neuroblastoma SHSY-5Y cells were used for β-III tubulin positive staining controls. Both U87MG and SHSY-5Y cells were grown in separate plates from the experimental cells; however, the cells were stained in parallel with the experimental plates for each antibody and were fixed and stained following the same protocol as the experimental cells. U87MG and SHSY-5Y cells were grown in a 24-well plate with DMEM/F12 + Glutamax media (Gibco, MA, USA) enriched with 10% heat-inactivated FBS (Sigma-Aldrich, MO, USA) until confluent.

Image analysis

For each stained plate, 10 randomised immunofluorescent images of each well were taken with a 20× objective using the GE Healthcare Life Sciences-IN Cell analyser 2200 high-content cellular analysis system. ImageJ 1.52p software was used for automated unbiased image analysis to count stained nuclei and positive stained area using threshold and analyse particles functions in a macro and create a ratio of stained area to number of nuclei. False positives and low-quality images (e.g., out of field, out of focus) were manually excluded from the analysis. Cell counts at each treatment were conducted using the same automated image analysis to count for cell nuclei for 20 fields of view at 20×.

Enzyme analysis

Protein extraction

Cell protein extraction protocol was adapted from Santos *et al.* 2017 (28). Cells were harvested by decanting culture media, rinsed twice in sterile 1× PBS and detached using a cell scraper and 1× PBS. The detached cells were then collected and centrifuged at 1,000 relative centrifugal force (rcf) for 5 minutes. The supernatant was decanted, and the cell pellet was frozen at –80 ℃ until ready for testing. Samples were defrosted on ice and resuspended in 10 µL of 1.5 M tris-HCL (hydrochloric acid) buffer. They were then pipette lysed on ice following 1min sonication in the sonicator bath.

Dot blots

CNPase plays an important role in myelin formation and oligodendrocyte development (29,30). To detect the presence of CNPase enzymes in the conditioned media, circles of 2 mm in diameter were drawn on the polyvinylidene difluoride (PVDF) membrane with graphite pencil, and the membrane was activated by wetting in methanol. It was then rinsed twice with 0.5 M Tris and then air dried. Subsequently, 2 µL of sample were added to the marked area and left to bind to the PVDF membrane. Once dry, it was rinsed in Tris-buffered saline, pH 7 (TBS) and blocked by washing 3 times, for 5–10 min each wash, in a solution of skim milk powder and MilliQ water (0.1% w/v). Then 2 µL of mouse anti-CNPase (1/200 Abcam, #ab6319) and rabbit anti-Glutaminase (1:1,000 Abcam, # ab156876) primary antibodies diluted in PBS was added to the respective marked areas and incubated at room temperature until absorbed. After, PVDF was rinsed 3 times for 5–10 min each wash with TBS; 2 µL of secondary antibody anti-mouse immunoglobulin G (IgG) alkaline phosphatase (1:30,000 A4312 Sigma-Aldrich) and Anti-rabbit IgG peroxidase (1:6,000 A6154 Sigma-Aldrich) was added to the marked areas and incubated at room temperature until absorbed. The PVDF was then collected and rinsed 3 times for 5–10 min each wash with TBS. The blot was then developed appropriately with 3',3-Diaminobenzidine tablets for developing peroxidase (D4293 Sigma-Aldrich) and BCIP/NBT for alkaline phosphatase (B5655 Sigma-Aldrich) and the blot was imaged.

CNPase enzyme assay

CNPase catalyses the hydrolysis of 2'3'-cAMP to 2'AMP (30,31). This reaction can be used to test for the presence or absence of functional CNPase enzyme secreted by the cells (*Figure 1*).

The methodology used was adapted from Dreiling and Mattson [1980], where CNPase + 2'3'-cAMP + Water + phenol red = 2'AMP + H^+ causing a decrease in pH that can be detected using a colourimetric assay (32). When

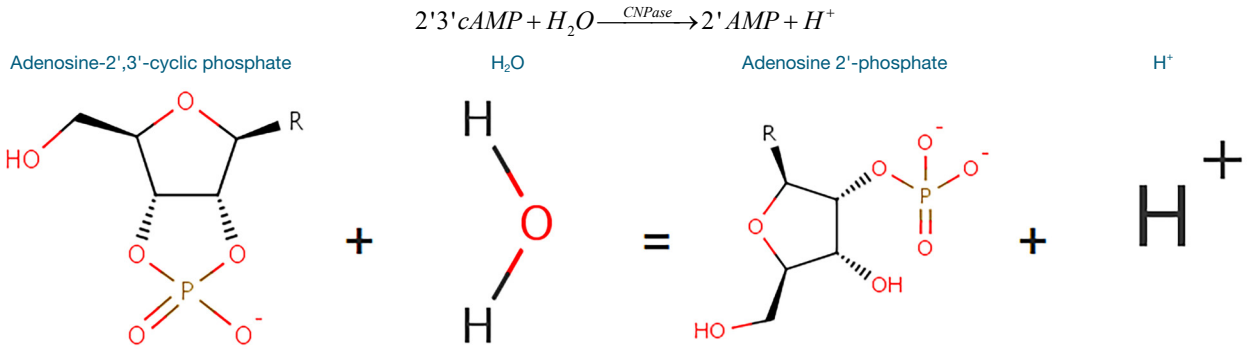

Figure 1 Chemical reaction used to detect the presence of functional CNPase. 2'3' cAMP and water in the presence of CNPase will be hydrolised to 2' AMP and hydrogen. AMP, adenosine 2'-phosphate.

CNPase activity increases, pH will decrease (32), and when measuring that pH change with phenol red at 560 nm, it will result in a drop in absorbance (33).

Cells were first lysed on ice by adding equal parts by volume of buffer (1.5 M tris-HCL buffer at pH 8.8) and cells with gentle pipetting. Following a subsequent sonication, 5 µL of cells were loaded into a 96 well plate with 5 µL of Phenol red at 1 mM in NaOH pH 8.4 with 40 µL of 2'3'-cAMP (Sigma-Aldrich) 15 mM in MiliQ water. Test samples consisted of cells treated with either B27, N2, C1 or DMEM and of conditioned media following 84 hrs incubation of ADSC with either B27, N2, C1, or DMEM. Absorbance was measured at 560 nm for 90 min with 30 min interval reads and then during a further overnight incubation with reads every hour in the TECAN Infinity 200 plate reader. The blanks included consisted of Phenol red at pH 8.4 + substrate for the cell blanks and of Phenol red at pH 8.4 + substrate + clean media (B27, N2, C1, DMEM). A colourimetric result indicates the presence of CNPase secreted by the ADSC. An increase from the baseline DMEM sample indicates that the cells are differentiating towards an oligodendrocytic cell lineage in the presence of a growth factor.

Statistical analysis

Data analysis for the raw imaging data was conducted using GraphPad Prism 8 using One-way analysis of variance (ANOVA), with a P value of <0.05 being considered statistically significant. Data analysis for Bioplex results was completed in R studio (version 1.3.959), where a single tail dendrogram heatmap was generated using Euclidean hierarchical clustering using R software for grouping cytokines trends over the different time points within each treatment.

Results

Cell culture

Cell morphology and survival

Morphological changes were observed between the treatments and the DMEM (undifferentiated control) (*Figure 2*) on both days 3.5 and 7. Individual cell morphology in the treatment groups becomes more polarised, and cells align more with each other in parallel bundles compared to the undifferentiated control cell organisation, specifically for B27 and N2 treatments. Cell counts did not significantly change between the treatments and the undifferentiated control DMEM (*Figure 2I*).

Immunocytochemistry and cellular differentiation

CNPase was not detected in undifferentiated cells and was expressed in all treatment groups (*Figures 3*,*4*), with the highest expression levels seen in the C1 group (*Figure 4A*) (P≤0.0001) and N2 group (*Figure 4B*) (P≤0.01). Doublecortin expression was absent in the undifferentiated ADSCs (*Figure 3B1*, *Figure 4B*) and only seen at low levels in the B27 and C1 treatment groups and significantly increased in the N2 treatment group (*Figure 3B3*, *Figure 4B*) (P≤0.0001). GFAP was absent in the undifferentiated ADSCs (*Figure 3C1*, *Figure 4C*), and GFAP levels were significantly increased in all treatment groups compared to the undifferentiated control (*Figure 3C2-C4*, *Figure 4C*) (P≤0.0001); however, these levels were lower than CNPase and Doublecortin expression levels in each treatment. b-III tubulin was expressed in the undifferentiated ADSCs (*Figure 3E1*) and did not significantly

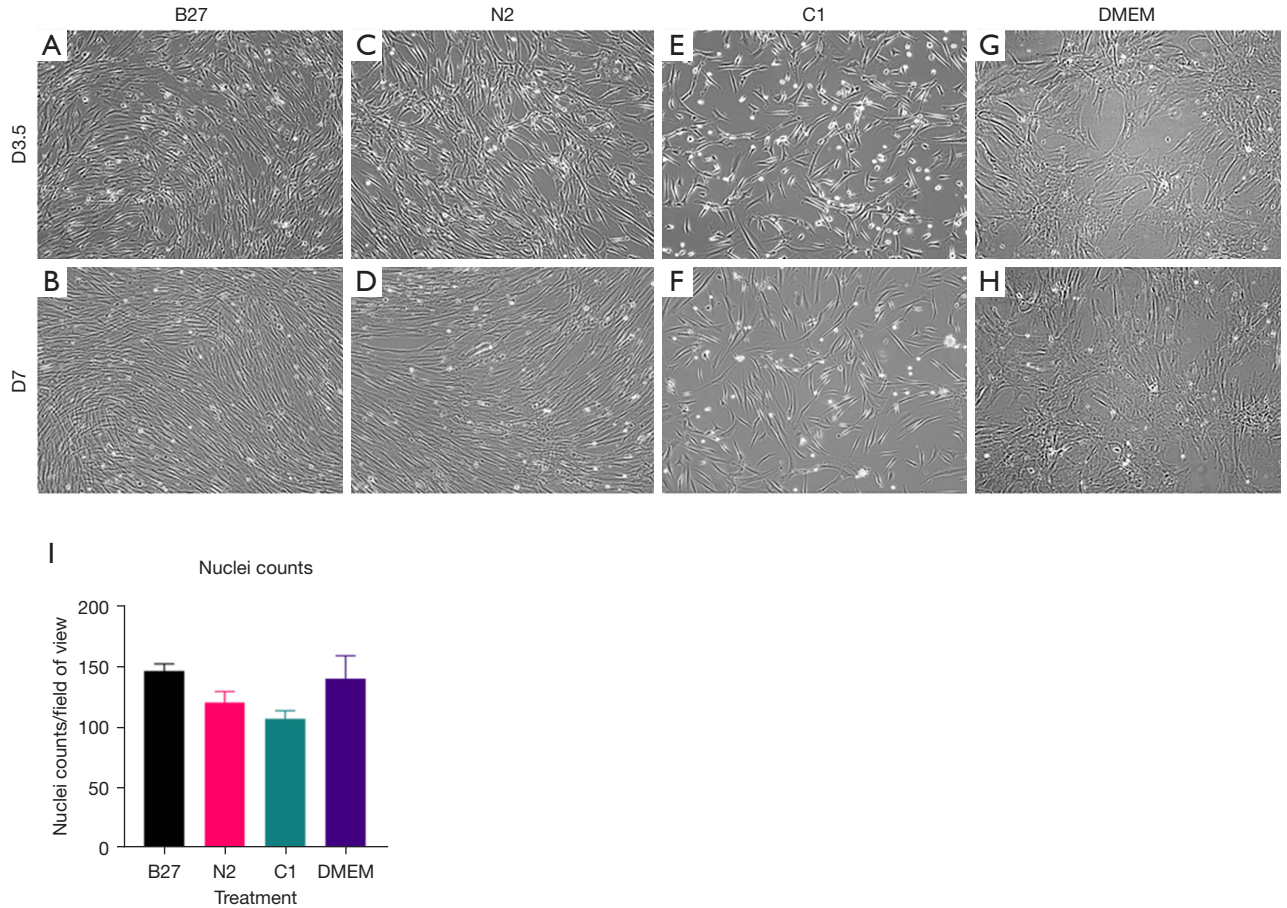

Figure 2 Cell morphology and nuclei analysis (A-H) phase images 10× at day 3.5 and day 7 of treatment with either; (A,B) B27; (C,D) N2; (E,F) C1; (G,H) DMEM (undifferentiated control). Representative of the 3 biological replicates. (I) Nuclei counts/field of view for each treatment group and DMEM (undifferentiated control) at D7 after treatment completion of the 3 biological triplicates. DMEM, Dulbecco's Modified Eagle medium.

increase following differentiation with any treatment (*Figure 3E2-E4*, *Figure 4D*) (P>0.05). Undifferentiated cells expressed high levels of Ki67 and are undergoing proliferation (*Figure 3D1*). This was similar to the proliferation levels seen in all treatment groups (*Figure 3D1-D4*, *Figure 4E*). Overall, immunocytochemistry results (*Figure 4*) show that while all treatments co-express all markers, C1 is the treatment that shows the highest levels of CNPase, followed by N2 with CNPase expression and the highest levels of Doublecortin.

Cytokine analysis

Bioplex

Bioplex assay was utilised to simultaneously investigate relative quantitative changes of 27 human cytokines across the different treatments and time points (*Figure 5*). The hierarchical clustering groups the cytokines with similar concentration trends over the treatment time points. Changes in cytokine levels for each treatment are shown as heatmaps in *Figure 4*. The heatmap provides an overview of all cytokines in relation to each other for each specific treatment over the two time points, day 3 and day 7, within each treatment.

The changes within each treatment can be observed on the heat maps (*Figure 5*). Overall, we find that IL-6, VEGF, and IL-8 cytokines continued to be the highest expressed cytokines regardless of treatment and IL-5 remained the cytokine with the lowest concentration across all treatments. However, when we look at differences between treatments on day 7 (*Figure 6*), it can be observed

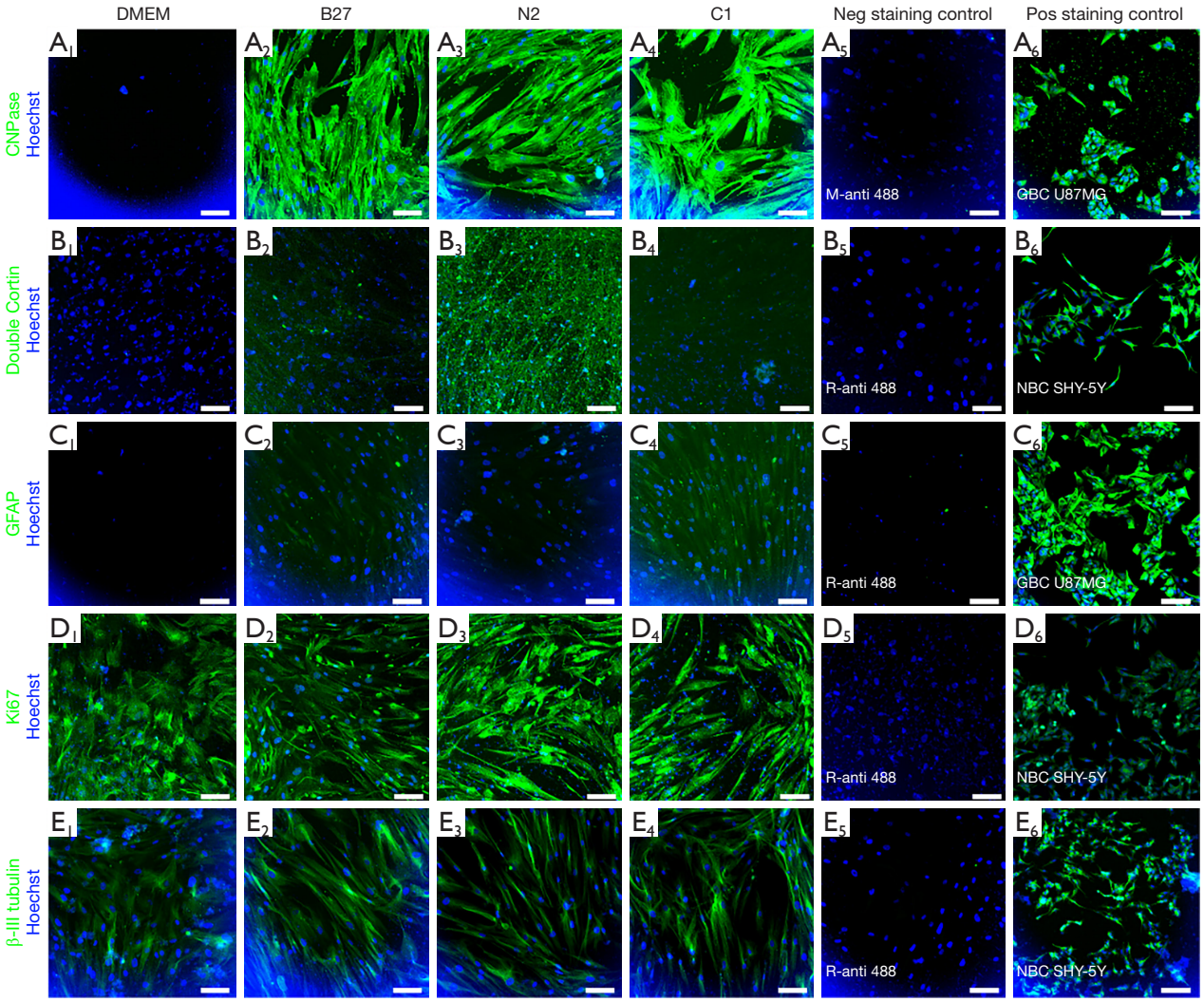

Figure 3 Immunocytochemistry staining for (A) CNPase, (B) DoubleCortin, (C) GFAP, (D) Ki67 and (E) β-III tubulin, and following 7-day differentiation using B27, N2, C1 *vs.* DMEM (undifferentiated control). Scale bars =100 µm. GFAP, glial fibrillary acidic protein; DMEM, Dulbecco's Modified Eagle medium.

that while the cytokines that were originally secreted in the highest concentrations in DMEM undifferentiated control stayed the highest secreted cytokine within each treatment when comparing treatments, C1 treatment had the lowest concentration of those cytokines. C1 treatment also showed a decrease in all cytokines compared to DMEM except in MCP-1, IL-8 G-CSF and GM-CSF cytokines, which showed an increase compared to DMEM. N2 treatment showed a similar cytokine expression pattern with several upregulated cytokines compared to undifferentiated hADSCs. N2 expressed increased GM-CSF, IL-8, GM-CSF, MCP-1, IL-7, IP-10, PDGF-BB, IL-17A, VEGF, MIP-1b, IL-2 and FGF basic.

The cytokines secreted in untreated ADSCs (DMEM control) stayed the highest within each treatment; however, the treatment that secreted the least of those cytokines was C1. Cytokines in C1 treatment decreased to those compared in DMEM. Additionally, when looking at the cytokine secretion trends, C1 and N2 treatments have a similar pattern, whereas B27 has an entirely different pattern of secretions.

In summary, a clear trend can be seen, with C1 being the treatment with an overall decrease in cytokine concentration over the 7-day treatment compared to DMEM.

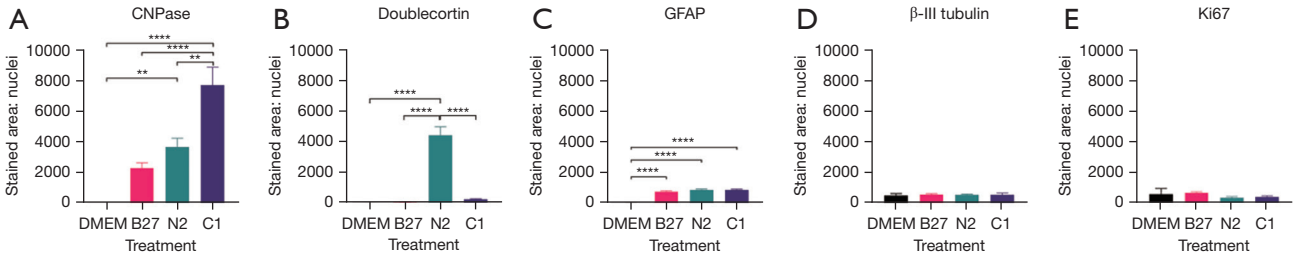

Figure 4 Immunocytochemistry marker expression by treatments DMEM, B27, N2, C1 following 7 days of treatment for (A) CNPase immunocytochemistry marker. All treatments showed increased CNPase compared to DMEM. However, only N2 and C1 showed to be significantly increased with **, P≤0.01 for N2 and ****, P≤0.0001. Overall, C1 treatment had the highest expression of CNPase (****, P≤0.0001 between C1 and b27, C1 and DMEM and **, P≤0.01 for C1 and N2). (B) Doublecortin immunocytochemistry maker. N2 treatment showed a significant increase of Doublecortin compared to all other treatments (****, P≤0.0001) (C) GFAP immunocytochemistry marker. All treatments showed significant increase in GFAP compared to DMEM (****, P≤0.0001) (D) β-III tubulin immunocytochemistry marker. There was no significant change between treatments. (E) Ki67 marker. There was no significant change between treatments. No statistical significance P>0.05; statistical significance *, P≤0.05; statistical significance **, P≤0.01; statistical significance ***, P≤0.001; statistical significance ****, P≤0.0001. DMEM, Dulbecco's Modified Eagle medium; GFAP, glial fibrillary acidic protein.

Enzyme analysis

Dot blot

The dot blot was used to detect any CNPase present in the media after treatment, indicative of CNPase secretion. *Figure 6* shows that there was little difference in CNPase secretion between all treatments. Day 3 (*Figure 7*) shows all treatments had higher CNPase secretion than DMEM undifferentiated control, whereas on day 7 (*Figure 8*), B27 and N2 CNPase secretion increased and C1 decreased by half.

CNPase assay

CNPase assay was conducted to detect the functionality of the CNPase enzyme present inside the cells as well as the CNPase enzyme secreted by the cells. When CNPase activity increases, it results in more H+ and, therefore, a drop in pH. The pH decrease changes phenol red from fuchsia to yellow, and that results in a descending gradient on the graphs (*Figure 8*).

In *Figure 6*, CNPase activity can be observed in both intercellular CNPase (*Figure 8A*) as well as extracellular CNPase (*Figure 8B*). C1 treatment shows the highest activity of CNPase over time intracellularly, while DMEM shows the highest activity of CNPase over time extracellularly.

Discussion

This study's hypothesis was that MSCs would commence differentiation towards neuronal-like lineage in all three treatments, given that B27, N2 and C1 are commercially available supplements used for neuronal differentiation and maintenance in neural cultures. However, when using these treatments on hADSCs, the results indicate that the cells may be differentiating towards different neural cell types under different growth conditions. Following treatment of hADSCs with B27, N2 and to a lesser extent C1, cells became polarised and aligned with one another; morphological changes indicative of neural differentiation. Additionally, cells survived and continued to proliferate as all cells were found to express Ki67 proliferation marker. Furthermore, immunocytochemistry results showed that cells in all treatments expressed some level of CNPase, a well-known oligodendrocyte marker, with C1 treatment expressing the highest levels of CNPase and all treatments increased GFAP to a lesser extent. N2 treated cells also expressed the neuronal marker doublecortin. Additionally, all cells, including undifferentiated hADSCs, expressed B-tubulin marker, a well-known early neuronal marker; however, the levels between undifferentiated cells and treated cells did not increase significantly. Cytokine levels following C1 treatment were reduced compared to the DMEM undifferentiated control in all cases but four: GM-CSF, IL-8, G-CSF and MCP-1. N2 showed a similar but reduced change compared to C1 except for FGF basic and IL-8. On the other hand, B27 presented a distinct cytokine expression pattern whereby most cytokines are upregulated except for RANTES, IL-12, 1L-13, IFN-g, IL-1ra, IL-10 and Eotaxin and where the upregulation or downregulation compared to DMEM undifferentiated control is not as

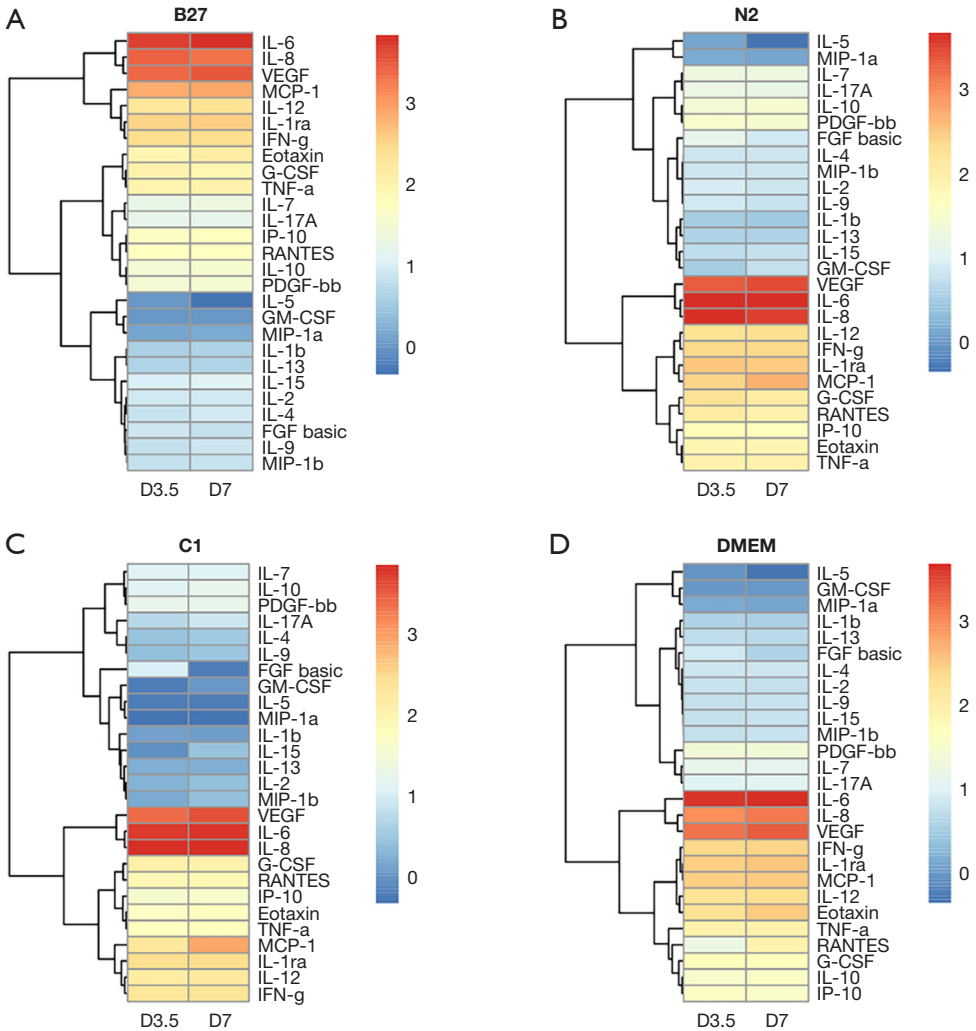

Figure 5 Hierarchical correlation and grouping of up/down regulated cytokines and interleukins from ADSCs temporal differentiation with B27, N2, C1 and DMEM (undifferentiated control). Cytokine concentration values were transformed to common logarithm values to normalize the data distribution. Values shown are Log [cytokine]. Cytokine expression trends were clustered using Hierarchical clustering by Euclidean test. Red: expression above median indicative of high cytokine concentration; blue: expression below the median indicative of lower cytokine concentration; yellow: median expression across all samples indicative of no change. All three relative to each other within that treatment. (A) Heatmap collecting Log10 of cytokine concentration and cytokine trends in B27. (B) Heatmap collecting Log10 of cytokine concentration and cytokine trends in N2. (C) Heatmap collecting Log10 of cytokine concentration and cytokine trends in C1. (D) Heatmap collecting Log10 of cytokine concentration and cytokine trends in DMEM (undifferentiated control). ADSCs, adipose-derived stem cell; IL, interlukine; VEGF vascular endothelial growth factor; MCP-1, monocyte chemoattractant protein-1; IFN-g, interferon gamma; G-CSF, granulocyte colony-stimulating factor; TNF-a, tumour necrosis factor alpha; IP-10, interferon gamma induced protein-10; PDGF, platelet-derived growth factor; GM-CSF, granulocyte-macrophage colony-stimulating factor; MIP, macrophage inflammatory protein; FGF basic, fibroblast growth factor basic; DMEM, Dulbecco's Modified Eagle medium.

notable as C1. The most notable finding of this study was the presence of high intracellular and extracellular levels of functional CNPase after a 7-day treatment with C1 and N2, and to a notable but lesser extent with B27.

CNPase expression is increased in hADSCs following C1, N2 and B27 treatment

Intracellular and extracellular functional CNPase was detected in all three treatments, with C1 having the

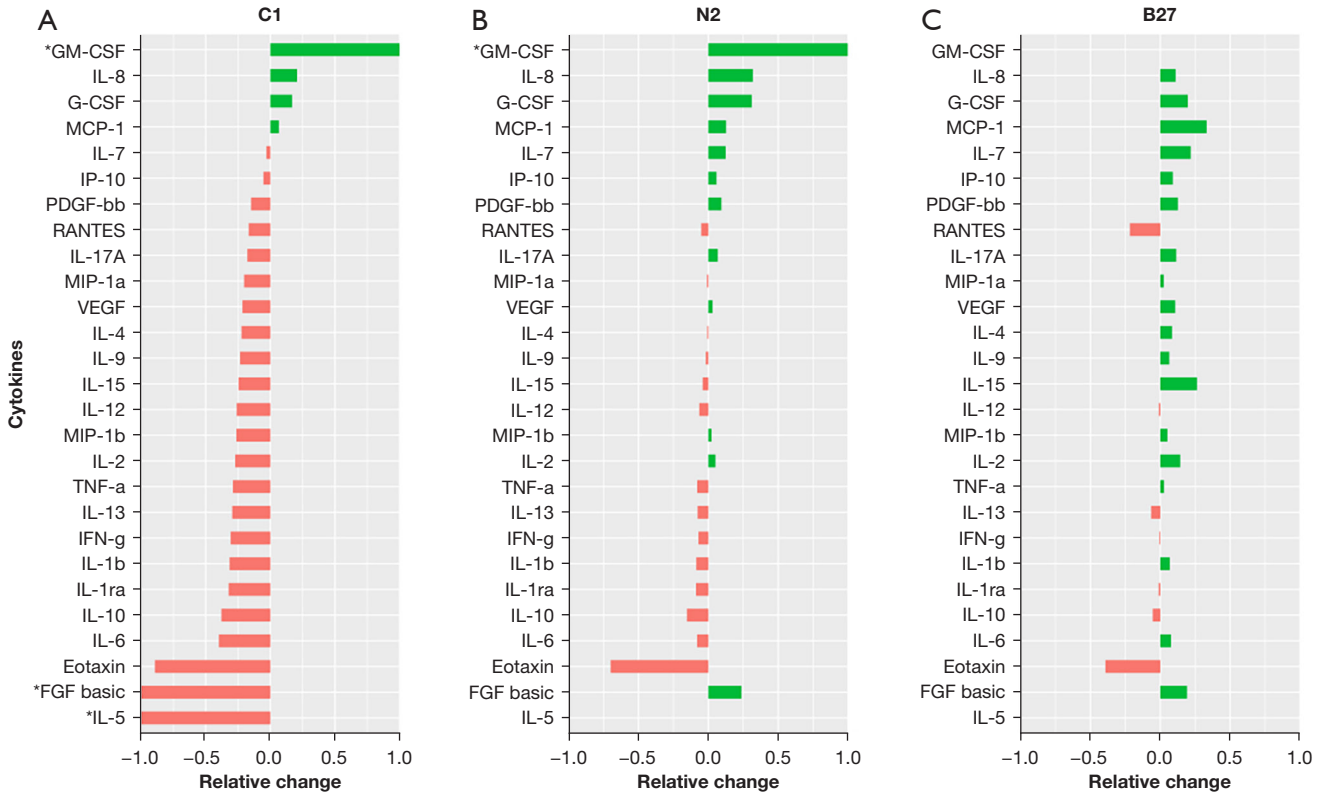

Figure 6 Cytokines' log10 concentration change relative to DMEM (negative control) at day 7. Grouped by treatment. Values were transformed into Log10 to graph the data. Cytokines marked with * resulted in -infinite and + infinite values when transformed as they showed a decrease to zero or an increase from zero. The graph correctly displays an increase or a decrease from baseline. Raw value concentration can be found in the supplementary data. (A) Log10 concentration change at day 7 for C1 treatment compared to DMEM; (B) Log10 concentration change at day 7 for N2 treatment compared to DMEM; (C) Log10 concentration change at day 7 for B27 treatment compared to DMEM. DMEM, Dulbecco's Modified Eagle medium.

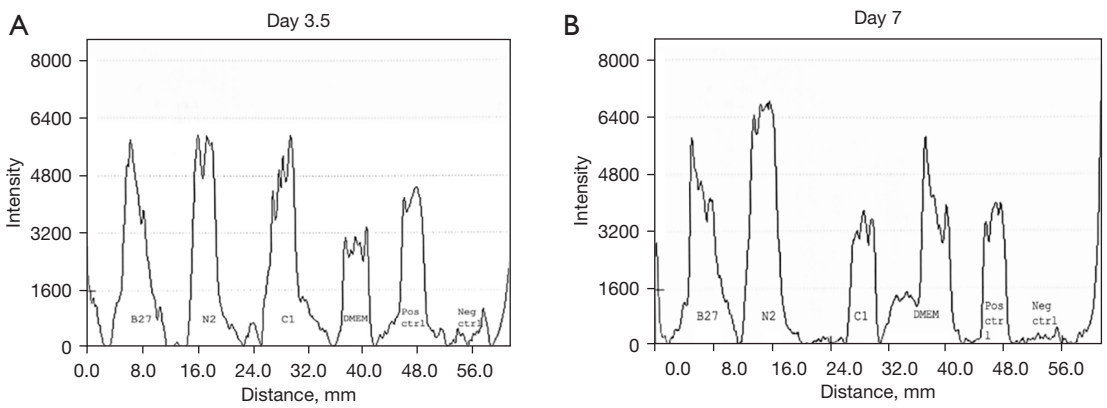

Figure 7 CNPase expression in treatment media supernatant. (A) CNPase expression in media supernatant at day 3.5 compared to DMEM undifferentiated control, a positive control, and a negative control (B) CNPase expression in media supernatant at day 7 compared to DMEM undifferentiated control, a positive control and a negative control. DMEM, Dulbecco's Modified Eagle medium.

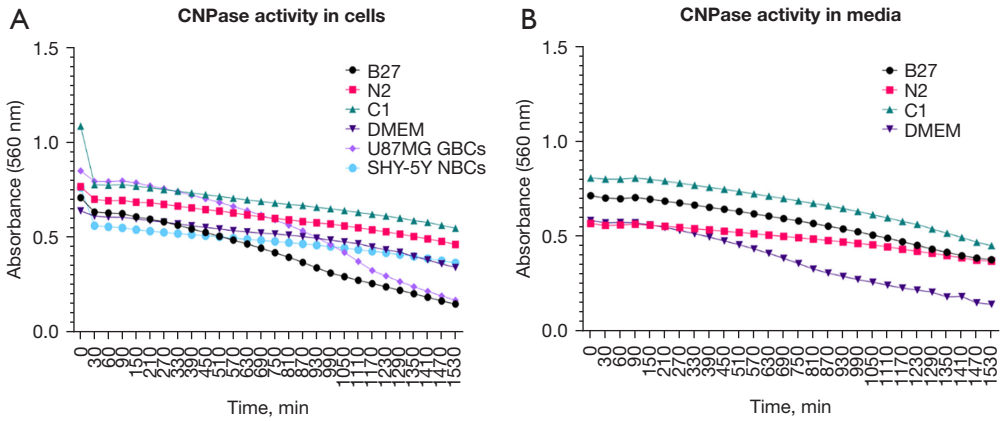

Figure 8 CNPase assay activity (A) CNPase activity in cells over 25 h. (B) CNPase activity in media over 25 h. Time intervals were first every 30 minutes for 90 minutes, and then every 60 minutes. DMEM, Dulbecco's Modified Eagle medium; GBC, glioblastoma cell; NBC, neuroblastoma cell.

highest expression of CNPase. Immunocytochemistry (*Figures 2,3*) showed that all treatments being investigated expressed markers indicative of commencement of neural differentiation. As seen in *Figures 2,3*, this change is most pronounced in C1, with the highest expression of CNPase and low levels of any other marker. Additionally, CNPase enzymatic assay results (*Figure 7*) showed that the cells expressed intracellular and secreted extracellular functional CNPase. CNPase is a well-established oligodendrocyte marker (29,30) that is mainly expressed in glial cells, with oligodendrocytes having the highest expression of this enzyme of the four major CNS cell types. This enzyme is necessary for oligodendrocyte development and branching and plays a critical role in early myelin formation (29) and neuronal health more generally (34). CNPase deficiency in the brain has been associated with multiple neurological diseases (31), including Down syndrome, Alzheimer's disease (35), and Multiple Sclerosis (36). Furthermore, it is a key component of the 2'3'-cAMP-Adenosine pathway responsible for the production of adenosine (30). Adenosine is a neuromodulator that increases significantly following injury and plays a role in neuroprotection post CNS injury (30,37-40). In the 2'3'-cAMP-Adenosine pathway, this occurs largely via CNPase present in the oligodendrocytes suggesting that oligodendrocytes have a role protecting the axons making CNPase a necessary enzyme for sustained function of the axon-myelin unit and for long-term axonal health (30). Furthermore, CNPase expression in MSCs has been previously seen in rodent cells. Rat ADSCs expressed CNPase marker after being treated with isobutylmethylxanthine (IBMX) induction (41). IBMX is a small molecule chemical that has since been successfully used in hADSCs neurodifferentiation inductions (19). Additionally, it has been observed that human foetal MSCs upregulate CNPase expression after exposure to oligodendrocyte differentiation medium (42) and that rat MSCs have a strong oligodendrogenic effect on rat neural progenitor cells (NPCs) (43). hADSCs have also shown increased CNPase expression after 2 week neural differentiation treatment with bFGF and forskolin (8), suggestive of the capacity for hADSCs to express CNPase marker as a sign of neuronal differentiation and supporting the idea that CNPase expression in hADSCs following treatment with B27, C1 and N2 is indicative of neural like differentiations especially oligodendrocytic lineage following C1 treatment.

CNPase expression is influenced by the presence of different cytokines

Cytokine changes are commonly seen following ADSC differentiation in a number of conditions (18,44,45). CNPase expression can also be influenced by the presence of different cytokines. Both IL-1b and TNF-a have been shown to inhibit the expression of CNPase in human oligodendrocytes (46). These two cytokines have been downregulated in C1 and N2, while they were upregulated in B27, consistent with the different levels of CNPase expression in the different treatments, with C1 having the highest expression and B27 having the least CNPase expression (*Figure 3*). Additionally, IL-8 has been shown to increase mouse oligodendrocyte

precursor proliferation as well as stimulate myelin basic protein *in vitro* (47), and this cytokine was upregulated in all treatments but particularly in C1 and N2 (*Figure 5*). G-CSF is another cytokine that was also found to be upregulated in all three treatments. Normally considered a growth factor for haematopoietic progenitor cells and neutrophils, it can also potentially be used for neural injury treatment such as spinal cord injury (48). G-CSF has been shown to protect oligodendrocytes from SCI-induced death by attenuating white matter loss and promoting functional recovery (49). G-CSF also has been shown to suppress the expression of pro-inflammatory cytokines IL-1b and TNF-a both *in vitro* (50,51) and *in vivo* (49,52); Therefore, G-CSF may have a role in upregulating CNPase expression indirectly through suppressing IL-1b and TNF-a given IL-1b, and TNF-a have been linked to CNPase expression suppression in human oligodendrocytes (46). Another cytokine that was upregulated in C1 and N2 is GM-CSF, generally associated with macrophage and eosinophil proliferation and maturation. This cytokine has also been shown to have neuroprotective effects in CNS diseases (53,54) and plays a role in NPC activation both *in vitro* and *in vivo* (55). Eotaxin-1 was found to be downregulated in all three treatments, with the most notable decrease in C1; Eotaxin is usually an immune modulator associated with the recruitment of eosinophils into inflammatory sites and is high in conditions such as asthma (56). It has recently been found to influence NPCs and microglia and can be secreted by several central nervous system cells (57). It is increased in neurodegenerative conditions such as schizophrenia and Alzheimer's disease (57,58) but appears to be active during accelerated aging and is stimulated by IL-4 and IL-13 (58), both of which are also downregulated in C1 and N2 treated ADSCs.

hADSCs differentiation differs following C1, N2 and B27 treatment

In the current experiments, the analysis showed that C1-treated hADSCs had the highest levels of functional intracellular CNPase, suggesting that they were actually differentiating towards the oligodendrocytic lineage. However, according to the manufacturer, C1 is reported to inhibit glial cell proliferation in primary neural cell cultures. hADSCs are of mesenchymal cell origin rather than nervous system origin. When treated with C1, they appear to downregulate common haemopoietic cytokines that are normally present in mesenchymal cell lines (as seen by a downregulation from the untreated cells in *Figure 6*), suggesting that the cells may be reverting from the mesenchymal to a less differentiated or neural-like lineage.

hADSCs treated with B27 presented the lowest expression of all immunocytochemistry markers (*Figures 2,3*) as well as the least CNPase activity in the CNPase enzymatic assay (*Figure 7*), indicative of the least neural differentiation. B27 is a very commonly used neural supplement; however, it is generally used for the long-term survival of neurons rather than initial commitment and differentiation (26,27). The hADSC treated with B27 did not express significantly higher levels of CNPase and doublecortin than the undifferentiated control cells and may not have developed expression of neural cell markers (CNPase and doublecortin) at these early time points. In contrast, N2 treatment showed mixed levels of neural differentiation, with similar levels of both CNPase and doublecortin. Doublecortin is a well-established marker for immature neurons and for neurogenesis (59-61). It is possible that N2 is showing a mixed population of cells given the expression of both CNPase and doublecortin markers or that the cells are co-expressing both markers; however, the co-expression of both CNPase and doublecortin has not been reported before. There were small increases of GFAP following incubation with all three supplements compared to the non-differentiated ADSCs. GFAP is typically used to identify mature astrocytes but in this short time frame and in the absence of large fold change it is unclear whether there is a robust differentiation pathway towards astrocytic lineage. However, GFAP expression even at low levels, in these mesenchymal ADSC does indicate an early neural differentiation, possible towards a more glial lineage (62).

Conclusions

Neural differentiation of hADSC can be successfully initiated using commonly available neuronal cell supplements C1 and N2. Although each supplement is usually used for neuronal differentiation and maintenance, we have shown that neural differentiation of hADSC can be initiated by these supplements with C1 pushing cells towards an oligodendrocytic lineage (increased CNPase) and N2 supporting neuronal differentiation (increased Doublecortin). B27 does not have a strong differentiating effect on hADSC at these early time points. Future work may investigate longer time intervals with further supplementation to further elucidate hADSC neural differentiation and would need to be

demonstrated in additional patient samples.

Acknowledgments

The authors would like to appreciate the Schwartz Foundation philanthropic donation to support research for partly funding the project, as well as Dr. Max L. Cummins for proofreading the article and helping with data visualisation and Carolina Zajc for proofreading the article.
Funding: This research was partially funded by the Schwartz Foundation philanthropic donation to support research.

Footnote

Conflicts of Interest: All authors have completed the ICMJE uniform disclosure form (available at https://sci.amegroups.com/article/view/10.21037/sci-2022-015/coif). The authors have no conflicts of interest to declare.

Ethical Statement: The authors are accountable for all aspects of the work in ensuring that questions related to the accuracy or integrity of any part of the work are appropriately investigated and resolved. The study was conducted in accordance with the Declaration of Helsinki (as revised in 2013). hADSCs from a single donor waste lipoaspirate were isolated and expanded with approval from the UTS Human Research Ethics Committee (Ethics No. 2013000437). Written informed consent was acquired for donor lipoaspirate release for research purposes only.

References

1. Tsuji W, Rubin JP, Marra KG. Adipose-derived stem cells: Implications in tissue regeneration. World J Stem Cells 2014;6:312-21.
2. Raposio E, Bonomini S, Calderazzi F. Isolation of autologous adipose tissue-derived mesenchymal stem cells for bone repair. Orthop Traumatol Surg Res 2016;102:909-12.
3. Wankhade UD, Shen M, Kolhe R, et al. Advances in Adipose-Derived Stem Cells Isolation, Characterization, and Application in Regenerative Tissue Engineering. Stem Cells Int 2016;2016:3206807.
4. Raposio E, Simonacci F, Perrotta RE. Adipose-derived stem cells: Comparison between two methods of isolation for clinical applications. Ann Med Surg (Lond) 2017;20:87-91.
5. Zuk PA, Zhu M, Mizuno H, et al. Multilineage cells from human adipose tissue: implications for cell-based therapies. Tissue Eng 2001;7:211-28.
6. Strioga M, Viswanathan S, Darinskas A, et al. Same or not the same? Comparison of adipose tissue-derived versus bone marrow-derived mesenchymal stem and stromal cells. Stem Cells Dev 2012;21:2724-52.
7. Gimble J, Guilak F. Adipose-derived adult stem cells: isolation, characterization, and differentiation potential. Cytotherapy 2003;5:362-9.
8. Jang S, Cho HH, Cho YB, et al. Functional neural differentiation of human adipose tissue-derived stem cells using bFGF and forskolin. BMC Cell Biol 2010;11:25.
9. Park J, Lee N, Lee J, et al. Small molecule-based lineage switch of human adipose-derived stem cells into neural stem cells and functional GABAergic neurons. Sci Rep 2017;7:10166.
10. Wislet-Gendebien S, Wautier F, Leprince P, et al. Astrocytic and neuronal fate of mesenchymal stem cells expressing nestin. Brain Res Bull 2005;68:95-102.
11. Foudah D, Monfrini M, Donzelli E, et al. Expression of neural markers by undifferentiated mesenchymal-like stem cells from different sources. J Immunol Res 2014;2014:987678.
12. Miwa H, Era T. Tracing the destiny of mesenchymal stem cells from embryo to adult bone marrow and white adipose tissue via Pdgfrα expression. Development 2018;145:dev155879.
13. Frese L, Dijkman PE, Hoerstrup SP. Adipose Tissue-Derived Stem Cells in Regenerative Medicine. Transfus Med Hemother 2016;43:268-74.
14. Rad AA, Heidari MH, Aliaghaei A, et al. In vitro differentiation of adipose derived stem cells into functional dopaminergic neurons. Biomedical and Pharmacology Journal. 2017;10:595-605.
15. Ahmadi N, Razavi S, Kazemi M, et al. Stability of neural differentiation in human adipose derived stem cells by two induction protocols. Tissue Cell 2012;44:87-94.
16. Soheilifar MH, Javeri A, Amini H, et al. Generation

of Dopamine-Secreting Cells from Human Adipose Tissue-Derived Stem Cells In Vitro. Rejuvenation Res 2018;21:360-8.
17. Faghih H, Javeri A, Amini H, et al. Directed differentiation of human adipose tissue-derived stem cells to dopaminergic neurons in low-serum and serum-free conditions. Neurosci Lett 2019;708:134353.
18. Santos J, Hubert T, Milthorpe BK. Valproic Acid Promotes Early Neural Differentiation in Adult Mesenchymal Stem Cells Through Protein Signalling Pathways. Cells 2020;9:619.
19. Fajardo J, Milthorpe BK, Santos J. Molecular Mechanisms Involved in Neural Substructure Development during Phosphodiesterase Inhibitor Treatment of Mesenchymal Stem Cells. Int J Mol Sci 2020;21:4867.
20. Rong JU, Wen Z, Rong WU, et al. Interaction between neural stem cells and bone marrow derived-mesenchymal stem cells during differentiation. Biomed Rep 2015;3:242-6.
21. Chi K, Fu RH, Huang YC, et al. Adipose-derived Stem Cells Stimulated with n-Butylidenephthalide Exhibit Therapeutic Effects in a Mouse Model of Parkinson's Disease. Cell Transplant 2018;27:456-70.
22. Carlson KB, Singh P, Feaster MM, et al. Mesenchymal stem cells facilitate axon sorting, myelination, and functional recovery in paralyzed mice deficient in Schwann cell-derived laminin. Glia 2011;59:267-77.
23. Wang L, Zhao Y, Pan X, et al. Adipose-derived stem cell transplantation improves learning and memory via releasing neurotrophins in rat model of temporal lobe epilepsy. Brain Res 2021;1750:147121.
24. Zhou F, Gao S, Wang L, et al. Human adipose-derived stem cells partially rescue the stroke syndromes by promoting spatial learning and memory in mouse middle cerebral artery occlusion model. Stem Cell Res Ther 2015;6:92.
25. Galindo LT, Filippo TR, Semedo P, et al. Mesenchymal stem cell therapy modulates the inflammatory response in experimental traumatic brain injury. Neurol Res Int 2011;2011:564089.
26. Brewer GJ, Torricelli J, Evege EK, et al. Neurobasal medium/B27 supplement: A new serum-free medium combination for survival of neurons. Focus 1994;16:6-9.
27. Brewer GJ, Torricelli JR, Evege EK, et al. Optimized survival of hippocampal neurons in B27-supplemented Neurobasal, a new serum-free medium combination. J Neurosci Res 1993;35:567-76.
28. Santos J, Milthorpe BK, Herbert BR, et al. Proteomic Analysis of Human Adipose Derived Stem Cells during Small Molecule Chemical Stimulated Pre-neuronal Differentiation. Int J Stem Cells 2017;10:193-217.
29. Raasakka A, Kursula P. The myelin membrane-associated enzyme 2',3'-cyclic nucleotide 3'-phosphodiesterase: on a highway to structure and function. Neurosci Bull 2014;30:956-66.
30. Verrier JD, Jackson TC, Gillespie DG, et al. Role of CNPase in the oligodendrocytic extracellular 2',3'-cAMP-adenosine pathway. Glia 2013;61:1595-606.
31. Jackson EK. Discovery and Roles of 2',3'-cAMP in Biological Systems. Handb Exp Pharmacol 2017;238:229-52.
32. Dreiling CE, Mattson C. A new spectrophotometric assay for 2',3'-cyclic nucleotide 3'-phosphohydrolase activity in nervous tissue. Anal Biochem 1980;102:304-9.
33. Rovati L, Fabbri P, Ferrari L, et al. Plastic Optical Fiber pH Sensor Using a Sol-Gel Sensing Matrix. Fiber Optic Sensors 2012:415-39.
34. Lappe-Siefke C, Goebbels S, Gravel M, et al. Disruption of Cnp1 uncouples oligodendroglial functions in axonal support and myelination. Nat Genet 2003;33:366-74.
35. Vlkolinský R, Cairns N, Fountoulakis M, et al. Decreased brain levels of 2',3'-cyclic nucleotide-3'-phosphodiesterase in Down syndrome and Alzheimer's disease. Neurobiol Aging 2001;22:547-53.
36. Walsh MJ, Murray JM. Dual implication of 2',3'-cyclic nucleotide 3' phosphodiesterase as major autoantigen and C3 complement-binding protein in the pathogenesis of multiple sclerosis. J Clin Invest 1998;101:1923-31.
37. Stone TW, Ceruti S, Abbracchio MP. Adenosine receptors and neurological disease: neuroprotection and neurodegeneration. Handb Exp Pharmacol 2009;(193):535-87.
38. Bell MJ, Kochanek PM, Carcillo JA, et al. Interstitial adenosine, inosine, and hypoxanthine are increased after experimental traumatic brain injury in the rat. J Neurotrauma 1998;15:163-70.
39. Robertson CL, Bell MJ, Kochanek PM, et al. Increased adenosine in cerebrospinal fluid after severe traumatic brain injury in infants and children: association with severity of injury and excitotoxicity. Crit Care Med 2001;29:2287-93.
40. Lauro C, Cipriani R, Catalano M, et al. Adenosine A1 receptors and microglial cells mediate CX3CL1-induced protection of hippocampal neurons against Glu-induced death. Neuropsychopharmacology 2010;35:1550-9.
41. Ning H, Lin G, Lue TF, et al. Neuron-like differentiation of adipose tissue-derived stromal cells and vascular smooth muscle cells. Differentiation 2006;74:510-8.

42. Kennea NL, Waddington SN, Chan J, et al. Differentiation of human fetal mesenchymal stem cells into cells with an oligodendrocyte phenotype. Cell Cycle 2009;8:1069-79.
43. Steffenhagen C, Dechant FX, Oberbauer E, et al. Mesenchymal stem cells prime proliferating adult neural progenitors toward an oligodendrocyte fate. Stem Cells Dev 2012;21:1838-51.
44. Santos J, Dalla PV, Milthorpe BK. Molecular Dynamics of Cytokine Interactions and Signalling of Mesenchymal Stem Cells Undergoing Directed Neural-like Differentiation. Life (Basel) 2022;12:392.
45. Razavi S, Razavi MR, Kheirollahi-Kouhestani M, et al. Co-culture with neurotrophic factor secreting cells induced from adipose-derived stem cells: promotes neurogenic differentiation. Biochem Biophys Res Commun 2013;440:381-7.
46. Jana M, Pahan K. Redox regulation of cytokine-mediated inhibition of myelin gene expression in human primary oligodendrocytes. Free Radic Biol Med 2005;39:823-31.
47. Kadi L, Selvaraju R, de Lys P, et al. Differential effects of chemokines on oligodendrocyte precursor proliferation and myelin formation in vitro. J Neuroimmunol 2006;174:133-46.
48. Takahashi H, Yamazaki M, Okawa A, et al. Neuroprotective therapy using granulocyte colony-stimulating factor for acute spinal cord injury: a phase I/IIa clinical trial. Eur Spine J 2012;21:2580-7.
49. Kadota R, Koda M, Kawabe J, et al. Granulocyte colony-stimulating factor (G-CSF) protects oligodendrocyte and promotes hindlimb functional recovery after spinal cord injury in rats. PLoS One 2012;7:e50391.
50. Nishiki S, Hato F, Kamata N, et al. Selective activation of STAT3 in human monocytes stimulated by G-CSF: implication in inhibition of LPS-induced TNF-alpha production. Am J Physiol Cell Physiol 2004;286:C1302-11.
51. Boneberg EM, Hareng L, Gantner F, et al. Human monocytes express functional receptors for granulocyte colony-stimulating factor that mediate suppression of monokines and interferon-gamma. Blood 2000;95:270-6.
52. Zavala F, Abad S, Ezine S, et al. G-CSF therapy of ongoing experimental allergic encephalomyelitis via chemokine- and cytokine-based immune deviation. J Immunol 2002;168:2011-9.
53. Bouhy D, Malgrange B, Multon S, et al. Delayed GM-CSF treatment stimulates axonal regeneration and functional recovery in paraplegic rats via an increased BDNF expression by endogenous macrophages. FASEB J 2006;20:1239-41.
54. Nakagawa T, Suga S, Kawase T, et al. Intracarotid injection of granulocyte-macrophage colony-stimulating factor induces neuroprotection in a rat transient middle cerebral artery occlusion model. Brain Res 2006;1089:179-85.
55. Hayashi K, Ohta S, Kawakami Y, et al. Activation of dendritic-like cells and neural stem/progenitor cells in injured spinal cord by GM-CSF. Neurosci Res 2009;64:96-103.
56. Conroy DM, Williams TJ. Eotaxin and the attraction of eosinophils to the asthmatic lung. Respir Res 2001;2:150-6.
57. Teixeira AL, Gama CS, Rocha NP, et al. Revisiting the Role of Eotaxin-1/CCL11 in Psychiatric Disorders. Front Psychiatry 2018;9:241.
58. Ivanovska M, Abdi Z, Murdjeva M, et al. CCL-11 or Eotaxin-1: An Immune Marker for Ageing and Accelerated Ageing in Neuro-Psychiatric Disorders. Pharmaceuticals (Basel) 2020;13:230.
59. Walker TL, Yasuda T, Adams DJ, et al. The doublecortin-expressing population in the developing and adult brain contains multipotential precursors in addition to neuronal-lineage cells. J Neurosci 2007;27:3734-42.
60. Vukovic J, Borlikova GG, Ruitenberg MJ, et al. Immature doublecortin-positive hippocampal neurons are important for learning but not for remembering. J Neurosci 2013;33:6603-13.
61. Couillard-Despres S, Winner B, Schaubeck S, et al. Doublecortin expression levels in adult brain reflect neurogenesis. Eur J Neurosci 2005;21:1-14.
62. Safford KM, Hicok KC, Safford SD, et al. Neurogenic differentiation of murine and human adipose-derived stromal cells. Biochem Biophys Res Commun 2002;294:371-9.

doi: 10.21037/sci-2022-015
Cite this article as: Pelegri NG, Milthorpe BK, Gorrie CA, Santos J. Neurogenic marker expression in differentiating human adipose derived adult mesenchymal stem cells. Stem Cell Investig 2023;10:7.